Anomalous thermal anisotropy of two-dimensional nanoplates of vertically grown MoS_2

Xiuqiang Li, Yueyang Liu, Qinghui Zheng, Xuejun Yan, Xin Yang, Guangxin Lv, Ning Xu, Yuxi Wang, Minghui Lu, Keqiu Chen, and Jia Zhu

Citation: Appl. Phys. Lett. **111**, 163102 (2017); doi: 10.1063/1.4999248
View online: http://dx.doi.org/10.1063/1.4999248
View Table of Contents: http://aip.scitation.org/toc/apl/111/16
Published by the American Institute of Physics

Anomalous thermal anisotropy of two-dimensional nanoplates of vertically grown MoS_2

Xiuqiang Li,[1,a)] Yueyang Liu,[2,a)] Qinghui Zheng,[1] Xuejun Yan,[1] Xin Yang,[1] Guangxin Lv,[1] Ning Xu,[1] Yuxi Wang,[1] Minghui Lu,[1] Keqiu Chen,[2,b)] and Jia Zhu[1,b)]
[1]*National Laboratory of Solid State Microstructures, College of Engineering and Applied Sciences and Collaborative Innovation Center of Advanced Microstructures, Nanjing University, Nanjing 210093, China*
[2]*School of Physics and Electronics, Hunan University, Changsha 410082, China*

(Received 7 August 2017; accepted 29 September 2017; published online 16 October 2017)

Heat flow control plays a significant role in thermal management and energy conversion processes. Recently, two dimensional (2D) materials with unique anisotropic thermal properties are attracting a lot of attention, as promising building blocks for molding the heat flow. Originated from its crystal structure, in most if not all the 2D materials, the thermal conductivity along the Z direction (k_z) is much lower than x-y plane thermal conductivity (k_{xy}). In this work, we demonstrate that 2D nanoplates of vertically grown molybdenum disulfide (VG MoS_2) can have anomalous thermal anisotropy, in which k_{xy} (about 0.83 W/m K at 300 K) is ~1 order of magnitude lower than k_z (about 9.2 W/m K at 300 K). Lattice dynamics analysis reveals that this anomalous thermal anisotropy can be attributed to the anisotropic phonon dispersion relations and the anisotropic phonon group velocities along different directions. The low k_{xy} can be attributed to the weak phonon coupling near the x-y plane interfaces. It is expected that this 2D nanoplates of VG MoS_2 with anomalous thermal anisotropy and low k_{xy} can serve as a complementary building block for device designs and advanced heat flow control. *Published by AIP Publishing.* https://doi.org/10.1063/1.4999248

Nanoscale heat flow control through material designs is critical for various energy conversion processes and thermal management.[1–6] Recently, there is growing interest in anisotropic thermal properties of two dimensional (2D) materials as it is not only fundamentally interesting[7–11] but also critical to many applications such as electronics,[12] thermoelectrics,[13,14] and thermal management.[15–20] The thermal anisotropy of 2D materials is fundamentally linked to their crystal structures. In most if not all of 2D materials, the thermal conductivity along the Z direction (k_z) is much lower than thermal conductivity within x-y plane (k_{xy}) primarily because of the much weaker van der Waals interactions between layers in the Z direction compared to the stronger covalent bonds between atoms in x-y plane.[21]

Here, we demonstrated that 2D nanoplates of vertically grown molybdenum disulfide [VG MoS_2, the schematic as shown Figs. 1(a) and 1(b)] can have anomalous thermal anisotropy with k_{xy} of 0.83 W/m K at 300 K, one order of magnitude lower than k_z (9.2 W/m K) at the same temperature. This k_{xy} of 2D nanoplates of VG MoS_2 is two orders of magnitude lower than that of normal 2D layered MoS_2 [about 100 W/m K at 300 K (Ref. 22)]. Finally, the physical mechanism for anomalous thermal anisotropy and low k_{xy} was also analyzed by using lattice dynamics and nonequilibrium molecular dynamics studies. It is expected that this 2D nanoplates of VG MoS_2 with anomalous thermal anisotropy and low k_{xy} can serve as a complementary building block for device designs and advanced heat flow control.

2D nanoplates of VG MoS_2 were synthesized by chemical vapor deposition using a horizontal tube furnace. First, the substrates (Si) were coated with 10–20 nm thick Mo film as a precursor by magnetron sputtering. Then, substrates are placed at the hot center of the tube furnace and sulfur (Sigma Aldrich) is placed at the upstream side. The tube is pumped to a pressure of about 60 Pa and flushed with Ar gas (100 sccm) to remove oxygen. Subsequently, the heating center of the tube furnace is raised to reaction temperature of 750 °C in 35 min, and the sulfur powder is kept at about 300 °C. The furnace is held at reaction temperature for 1 h, followed by natural cool-down. Finally, the VG MoS_2 film was obtained. For exfoliation, the VG MoS_2 film with substrate was put into deionized water followed by ultrasound (100 W, 5 min). Then, we can drip the solution with 2D nanoplates of VG MoS_2 to other substrates, and obtain 2D nanoplates of VG MoS_2 after volatilization of water.

The morphologies and structures of 2D nanoplate of VG MoS_2 were characterized by transmission electron microscopy (JEM-200CX) and Raman spectroscopy (WITEC Raman spectrometer). The thickness of 2D nanoplate of VG MoS_2 was measured by AFM (Cypher S, Oxford instruments) on thermal measurement devices.

The anomalous thermal anisotropy and low k_{xy} of 2D nanoplates of VG MoS_2 is linked to its structure, achieved by a unique process. The VG MoS_2 films [as shown in Fig. 1(c)] are converted from magnetron sputtered, ultrathin Mo films (10–20 nm thick) through a rapid sulfurization process in a horizontal tube furnace, where sulfur powders are used as the precursors (for more details, see above paragraph).[23] Because of this sulfurization process, 2D nanoplates of VG MoS_2 have several unique structures, very different from

[a)]X. Li and Y. Liu contributed equally to this work.
[b)]Electronic addresses: keqiuchen@hnu.edu.cn and jiazhu@nju.edu.cn.

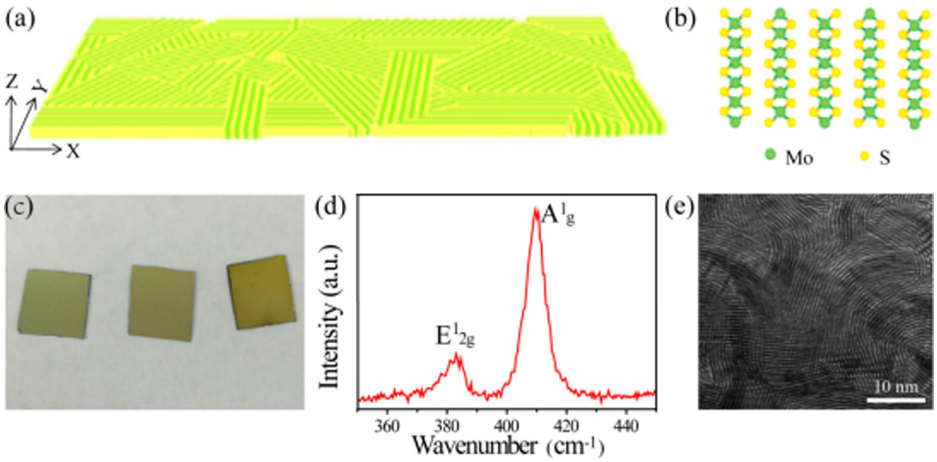

FIG. 1. (a) Schematic of VG MoS_2. (b) Side-view of VG MoS_2. (c) Optical image of 2D nanoplates of VG MoS_2 with different thicknesses on substrate (about 1 cm × 1 cm). (d) Raman spectra of 2D nanoplates of VG MoS_2. (e) TEM image of 2D nanoplates of VG MoS_2.

normal layered MoS_2 and other 2D materials. First, as shown in the schematics [Fig. 1(a)], the VG MoS_2 is composed of vertically aligned layers [in other words, the layers are aligned along Z direction, perpendicular to the substrate, as shown in Fig. 1(b)]. The structures of vertically aligned layers are confirmed by Raman spectra [Fig. 1(d)] and TEM image [Fig. 1(e)] discussed as below. In Raman spectra, E^1_{2g} (x-y plane vibration mode) and A^1_{1g} (Z direction vibration mode) of MoS_2 are, respectively, assigned to be ~383 and ~408 cm^{-1}.[23,24] As shown in Fig. 1(d), the intensity ratio of E^1_{2g}/A^1_{1g} is as low as ~0.25, which indicates the domination of vertical growth and exposed MoS_2 edge sites.[24] Second, as demonstrated in the high resolution TEM image [Fig. 1(e)], 2D nanoplates of VG MoS_2 are polycrystalline with nanometer-scale grain size. Therefore, it is clear that this 2D nanoplates is composed of densely packed, all vertically aligned 2D MoS_2 layers. These unique crystal structures of 2D nanoplates of VG MoS_2 can enable anomalous thermal anisotropy and low k_{xy}, as explained in more details below.

For thermal conductivity measurement, 2D nanoplates of VG MoS_2 can be exfoliated from substrates through ultrasound (for more details, see the above paragraph). The typical morphologies and thickness of the VG MoS_2 plate after exfoliation are shown in Figs. 2(a) and 2(b), respectively. As shown in Figs. 2(a), 2D nanoplates of VG MoS_2 with about a few hundred micron square area can be obtained after exfoliation. The thickness of 2D nanoplates of VG MoS_2 is about nanometer thick, and can be tuned by the thickness of initial Mo film (2D nanoplate of VG MoS_2 with different thicknesses can be found in supplementary material, S I). The corresponding optical image of 2D nanoplates of VG MoS_2 on suspended thermal measurement device after transfer is shown in Fig. 2(c).

The k_{xy} and k_z of 2D nanoplate of VG MoS_2 were measured with suspended micro-bridge device[25–30] and time-domain thermoreflectance (TDTR),[31] respectively (see supplementary material, S II for more details). As shown in Fig. 3(a), the k_{xy} and k_z of 2D nanoplate of VG MoS_2 are ~0.83 and ~9.2 W/m K at 300 K, respectively. As we know, for almost all the 2D materials, k_z is much lower than k_{xy} because of the much weaker van der Waals interactions between layers along the Z direction compared to the stronger covalent bonds between atoms in x-y plane. The anomalous thermal

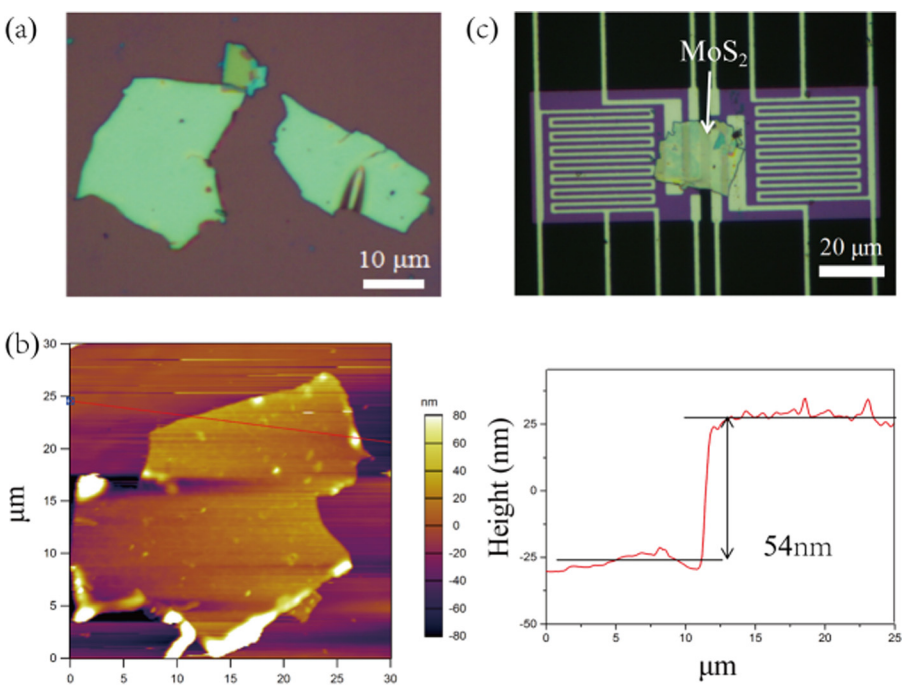

FIG. 2. (a) Optical image of 2D nanoplates of VG MoS_2 on substrate. (b) AFM image of 2D nanoplates of VG MoS_2. (c) Optical image of 2D nanoplates of VG MoS_2 on suspended pads.

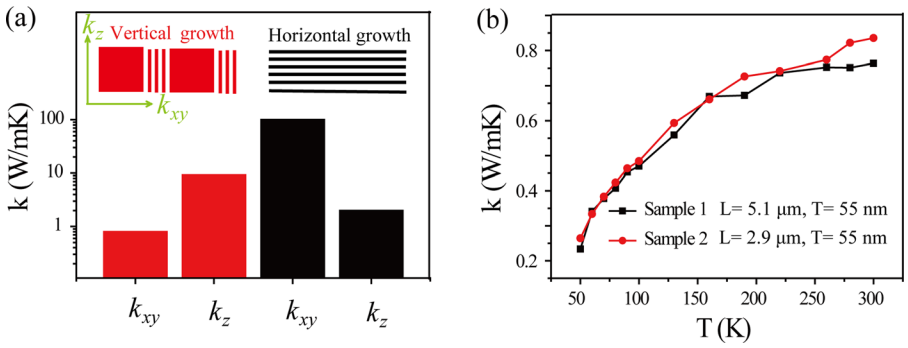

FIG. 3. (a) Thermal conductivity of MoS_2 with different structures at 300 K. More details about referenced thermal conductivity of horizontal growth MoS_2 can be found in Ref. 22. (b) k_{xy} of 2D nanoplate of VG MoS_2 (where L and T denote as length and thickness, respectively).

anisotropy of 2D nanoplates of VG MoS_2 ($k_{xy}/k_z = 11$) is clear, compared to traditional MoS_2 ($k_{xy}/k_z = 0.02$[22]) which can be attributed to the anisotropic phonon dispersion relations and the anisotropic phonon group velocities, as explained in more details below.

It is also interesting that the k_{xy} of 2D nanoplate of VG MoS_2 is very low, and thus the systematic thermal measurements were employed. As shown in Fig. 3(b), The k_{xy} of 2D nanoplate of VG MoS_2 increases from ~0.26 (50 K) to ~0.83 W/m K (300 K) with increasing temperature (the analysis of thermal contact resistance can be found in supplementary material, S III). It is about two orders lower than k_{xy} of normal layered MoS_2 [100 W/m K at 300 K (Ref. 22)] and even about three times lower than the k_z of normal layered MoS_2 [2 W/m K at 300 K (Ref. 32)]. Scatterings related to phonon-boundary and phonon-defects are the two possible reasons for low k_{xy} of 2D nanoplate of VG MoS_2. It has been reported in the literature, phonon-defects scattering can reduce the k_{xy} of MoS_2 [the thermal conductivity can be reduced about 2× when the defect concentration is 0.25% (Ref. 33)] the dramatic reduction (about two order of magnitude lower than normal layered MoS_2) can be mainly ascribed to phonon-boundary scattering. Hence, it is expected that the low k_{xy} of 2D nanoplate of VG MoS_2 can be attributed to the weak phonon coupling near the x-y plane interfaces (as explained in more details below).

To further illustrate the underlying mechanism of the thermal anisotropy and the low k_{xy} of 2D nanoplate of VG MoS_2, we investigate its direction-dependent lattice vibration by using lattice dynamics and nonequilibrium molecular dynamics studies (for more details about model preparation, see supplementary material, S IV). We first build a small unit cell of 2D nanoplate of VG MoS_2 shown in the inset of Fig. 4(a) to check the phonon dispersion curves and the group velocities along different directions. It is seen in Figs. 4(a) and 4(b) that the phonon dispersion along the X direction (within the x-y plane) and the Z direction (perpendicular to the x-y plane) differs greatly with each other. The acoustic branches along the X direction grows much slower than that of the Z direction, and the optical branches along the X

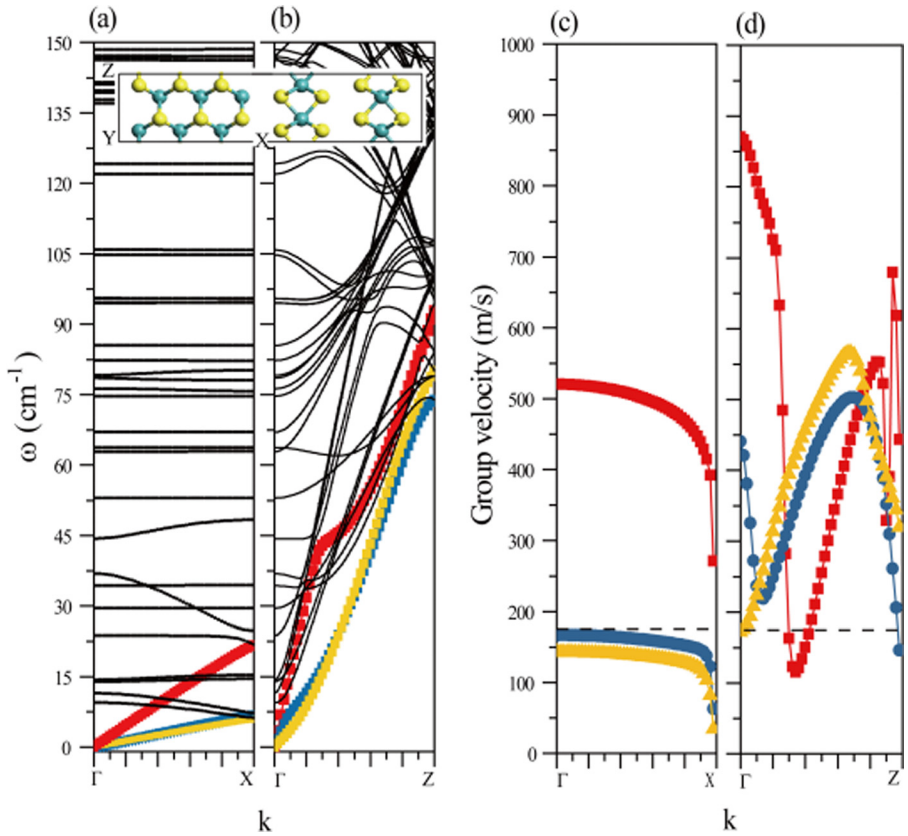

FIG. 4. (a) and (b) Dispersion curves along the X and Z directions, the acoustic branches are colored specially by red, blue, and yellow. The inset shows the unit cell and the primitive vectors. (c) and (d) The group velocities of the acoustic phonons along the X and Z directions.

direction are mostly flat while that along the Z direction increases sharply with the wave vector. Since the slope of the acoustic dispersion relation ($\partial\omega/\partial k$) is the phonon group velocity, and the group velocity is a key factor for thermal conductivity, we can calculate the phonon group velocity along different directions to examine the thermal anisotropy. Figures 4(c) and 4(d) show the phonon group velocity along the X direction and Z direction, respectively. The group velocity along the X direction is found to be very uniform because the dispersion curves along the X direction are nearly straight. In contrast, the dispersion curves along the Z direction are twisty, and thus the corresponding group velocity presents several twists and turns. Nevertheless, it is clearly seen that the group velocity of the two lower acoustic branches along the X direction is always much smaller than that along the Z direction, and thus contribute greatly to the thermal anisotropy. Besides, the upper branch along the X direction also presents much smaller group velocity except at the middle wave vector range. All these results suggest the existence of thermal anisotropy, and explain the low k_{xy} in 2D nanoplate of VG MoS_2.

Focusing on the x-y plane thermal transport, we calculate the vibrational density of states (VDOS) of the atoms around the interface to show the phonon scattering within the x-y plane. A model that consists of two segments is built and shown in Fig. 5(a). The two segments are designed to be perpendicular to each other and vertical to the x-y plane to resemble the experimentally grown samples. To generate a heat flow through the hybrid structure, the Nose-Hoover thermostat is utilized to keep the temperature of the left and the right end at 350 K and 250 K, respectively. A thermal transport progress is then triggered, and many thermal quantities including temperature, heat flux, and vibration frequencies and so on can be statistically collected.

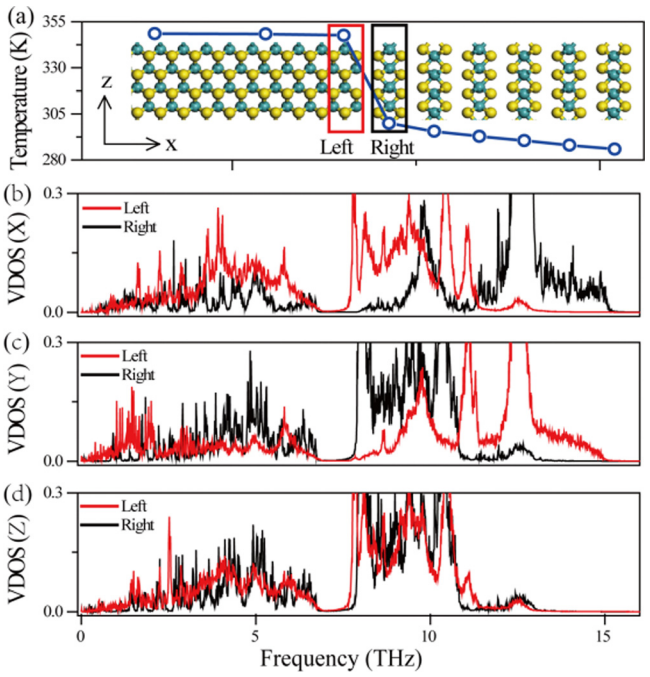

FIG. 5. (a) Model and temperature distribution. (b)–(d) VDOS along the X, Y, and Z directions. The structure grows along the Y direction.

With the VDOS of certain atom groups, we can not only figure out at which frequencies the atoms are vibrating but also determine whether the heat transfer is easy or not by comparing the VDOS of adjacent atom groups. For example, the change of the VDOS has been used to explain the decrease of thermal conductivity,[34] and the match or mismatch of the VDOS has been widely used to explain the thermal rectification effect in nanostructures.[35,36] As shown in Figs. 5(b)–5(d), the VDOS of the two interfacial atom groups are put together to show their matching degree, and the comparison is made for all the three directions to show the anisotropy. It is clearly seen that the VDOS of the two atom groups matches well only along the Z direction, and they differ with each other along the X direction and the Y direction greatly at both low-frequency range and high-frequency range. The mismatch of the VDOS will undoubtedly result in low phonon coupling near the interface, and induce the reduction of thermal conductivity and an abrupt temperature drop that can be seen in Fig. 5(a). The perfect match of the VDOS along the Z direction, on the other hand, will facilitate the thermal transport. These results explain the low k_{xy}, and illustrate the thermal anisotropy of 2D nanoplate of VG MoS_2.

We demonstrated anomalous thermal anisotropy in this structure in 2D nanoplate of VG MoS_2. The results showed that the k_{xy} with 0.83 W/m K is $\sim 11\times$ lower than k_z with 9.2 W/m K at 300 K. Lattice dynamics analysis reveals that this anomalous thermal anisotropy can be attributed to the anisotropic phonon dispersion relations and the anisotropic phonon group velocities. The low k_{xy} can be attributed to the weak phonon coupling near the x-y plane interfaces. A material with anomalous thermal anisotropy can serve as a complementary building block for device design that can conduct heat along the Z direction instead of the XY direction, which prevent the generation of hotspot, protect neighboring thermolabile device, and therefore enable advanced heat flow control. We expect that the reveal of thermal transport properties of 2D nanoplate of VG MoS_2 not only can broaden its potential applications in heat flow control, but also provide complementary building blocks for designing devices.

See supplementary material for the thickness characteristic of 2D nanoplate of VG MoS_2, thermal measurement, calculation of thermal contact resistance, and model preparation.

We acknowledge the micro-fabrication center of National Laboratory of Solid State Microstructures (NLSSM) for technique support. This work was jointly supported by the National Key Research and Development Program of China (Grant No. 2017YFA0205700) and the State Key Program for Basic Research of China (Grant No. 2015CB659300), National Natural Science Foundation of China (Grant Nos. 11621091 and 11574143), Natural Science Foundation of Jiangsu Province (Grant No. BK20150056), the Project Funded by the Priority Academic Program Development of Jiangsu Higher Education Institutions (PAPD), and the Fundamental Research Funds for the Central Universities (Grant Nos. 021314380068, 021314380089, and 021314380091).

[1]N. B. Li, J. Ren, L. Wang, G. Zhang, P. Hänggi, and B. W. Li, Rev. Mod. Phys. **84**(3), 1045 (2012).
[2]B. Li, L. Wang, and G. Casati, Phys. Rev. Lett. **93**(18), 184301 (2004).
[3]J. Zhu, K. Hippalgaonkar, S. Shen, K. Wang, Y. Abate, S. Lee, J. Wu, X. Yin, A. Majumdar, and X. Zhang, Nano Lett. **14**(8), 4867 (2014).
[4]S. Liu, P. Hanggi, N. Li, J. Ren, and B. Li, Phys. Rev. Lett. **112**(4), 040601 (2014).
[5]D. G. Cahill, P. V. Braun, G. Chen, D. R. Clarke, S. H. Fan, K. E. Goodson, P. Keblinski, W. P. King, G. D. Mahan, A. Majumdar, H. J. Maris, S. R. Phillpot, E. Pop, and L. Shi, Appl. Phys. Rev. **1**(1), 011305 (2014).
[6]A. I. Hochbaum, R. Chen, R. D. Delgado, W. Liang, E. C. Garnett, M. Najarian, A. Majumdar, and P. Yang, Nature **451**(7175), 163 (2008).
[7]Q. Fu, J. K. Yang, Y. F. Chen, D. Y. Li, and D. Y. Xu, Appl. Phys. Lett. **106**(3), 031905 (2015).
[8]C. Muratore, V. Varshney, J. J. Gengler, J. Hu, J. E. Bultman, A. K. Roy, B. L. Farmer, and A. A. Voevodin, Phys. Chem. Chem. Phys. **16**(3), 1008 (2014).
[9]S. Lee, F. Yang, J. Suh, S. Yang, Y. Lee, G. Li, H. Sung Choe, A. Suslu, Y. Chen, C. Ko, J. Park, K. Liu, J. Li, K. Hippalgaonkar, J. J. Urban, S. Tongay, and J. Wu, Nat. Commun. **6**, 8573 (2015).
[10]Y. Xu, X. Chen, B. Gu, and W. Duan, Appl. Phys. Lett. **95**(23), 233116 (2009).
[11]T. Liu, Y. Chen, C. Pao, and C. Chang, Appl. Phys. Lett. **104**(20), 201909 (2014).
[12]F. Xia, H. Wang, and Y. Jia, Nat. Commun. **5**, 4458 (2014).
[13]L. D. Zhao, S. H. Lo, Y. Zhang, H. Sun, G. Tan, C. Uher, C. Wolverton, V. P. Dravid, and M. G. Kanatzidis, Nature **508**(7496), 373 (2014).
[14]R. Q. Guo, X. J. Wang, Y. D. Kuang, and B. L. Huang, Phys. Rev. B **92**, 115202 (2015).
[15]B. Wicklein, A. Kocjan, G. Salazar-Alvarez, F. Carosio, G. Camino, M. Antonietti, and L. Bergstrom, Nat. Nanotechnol. **10**(3), 277 (2015).
[16]M. Smalc, G. Shives, G. Chen, S. Guggari, J. Norley, and R. A. Reynolds, Proceedings IPACK2005, San Francisco, California, July 17–22, Paper number: IPACK2005-73073, 2005.
[17]C. Chen, Y. Li, J. Song, Z. Yang, Y. Kuang, E. Hitz, C. Jia, A. Gong, F. Jiang, J. Zhu, B. Yang, J. Xie, and L. Hu, Adv. Mater. **29**, 1701756 (2017).
[18]Y. Li, T. Gao, Z. Yang, C. Chen, W. Luo, J. Song, E. Hitz, C. Jia, Y. Zhou, B. Liu, B. Yang, and L. Hu, Adv. Mater. **29**, 1700981 (2017).
[19]X. Li, W. Xu, M. Tang, L. Zhou, B. Zhu, S. Zhu, and J. Zhu, Proc. Natl. Acad. Sci. **113**(49), 13953 (2016).
[20]X. Li, R. Lin, G. Ni, N. Xu, X. Hu, B. Zhu, G. Lv, J. Li, S. Zhu, and J. Zhu, "Graphene Oxide-Based Evaporator with One-Dimensional Water Transport Enabling High- Efficiency Solar Desalination," Nano Energy (published online, 2017).
[21]Y. Wang, N. Xu, D. Li, and J. Zhu, Adv. Funct. Mater. **27**(19), 1604134 (2017).
[22]G. Zhu, J. Liu, Q. Zheng, R. Zhang, D. Li, D. Banerjee, and D. G. Cahill, Nat. Commun. **7**, 13211 (2016).
[23]D. Kong, H. Wang, J. J. Cha, M. Pasta, K. J. Koski, J. Yao, and Y. Cui, Nano Lett. **13**(3), 1341 (2013).
[24]Y. W. Jung, J. Shen, Y. H. Liu, J. M. Woods, Y. Sun, and J. J. Cha, Nano Lett. **14**(12), 6842 (2014).
[25]I. Jo, M. T. Pettes, J. Kim, K. Watanabe, T. Taniguchi, Z. Yao, and L. Shi, Nano Lett. **13**(2), 550 (2013).
[26]L. Shi, D. Li, C. Yu, W. Jang, D. Kim, Z. Yao, P. Kim, and A. Majumdar, J. Heat Transfer **125**(5), 881 (2003).
[27]H. Tang, X. Wang, Y. Xiong, Y. Zhao, Y. Zhang, Y. Zhang, J. Yang, and D. Xu, Nanoscale **7**(15), 6683 (2015).
[28]J. Yang, Y. Yang, S. W. Waltermire, X. Wu, H. Zhang, T. Gutu, Y. Jiang, Y. Chen, A. A. Zinn, R. Prasher, T. T. Xu, and D. Li, Nat. Nanotechnol. **7**(2), 91 (2011).
[29]X. Xu, L. F. Pereira, Y. Wang, J. Wu, K. Zhang, X. Zhao, S. Bae, C. Tinh Bui, R. Xie, J. T. Thong, B. H. Hong, K. P. Loh, D. Donadio, B. Li, and B. Ozyilmaz, Nat. Commun. **5**, 3689 (2014).
[30]C. Wang, J. Guo, L. Dong, A. Aiyiti, X. Xu, and B. Li, Sci. Rep. **6**, 25334 (2016).
[31]D. G. Cahill, Rev. Sci. Instrum. **75**, 5119 (2004).
[32]J. Liu, G. Choi, and D. G. Cahill, J. Appl. Phys. **116**(23), 233107 (2014).
[33]Z. W. Ding, Q. X. Pei, J. W. Jiang, and Y. W. Zhang, J. Phys. Chem. C **119**(28), 16358 (2015).
[34]M. Hu, K. P. Giapis, J. V. Goicochea, X. Zhang, and D. Poulikakos, Nano Lett. **11**(2), 618 (2011).
[35]J. Lee, V. Varshney, A. K. Roy, J. B. Ferguson, and B. L. Farmer, Nano Lett. **12**(7), 3491 (2012).
[36]Y. Y. Liu, W. X. Zhou, and K. Q. Chen, Sci. Rep. **5**, 17525 (2015).